PAPER

Frequency-dependent radiation properties of negative permittivity metamaterial reflector antenna

IOP Publishing Physica Scripta
Phys. Scr. 94 (2019) 105811 (9pp) https://doi.org/10.1088/1402-4896/ab2655

Frequency-dependent radiation properties of negative permittivity metamaterial reflector antenna

Jovia Jose[1], Sikha K Simon, Joe Kizhakooden[2], Anju Sebastian, Sreedevi P Chakyar, Nees Paul[2], Bindu C, Jolly Andrews and V P Joseph

Christ College (Autonomous), Irinjalakuda, University of Calicut , Kerala, India

E-mail: vpj@christcollegeijk.edu.in

Received 21 December 2018, revised 9 May 2019
Accepted for publication 3 June 2019
Published 7 August 2019

Abstract

This paper reports a novel type of microwave reflector antenna that uses the frequency-dependent properties of an epsilon negative (ENG) metamaterial medium. The frequency-dependent characteristics of this artificial plasma medium is analyzed using the dispersive auxiliary differential equation finite difference time domain (ADE-FDTD) method by employing a Gaussian pulse and the results are verified experimentally using an artificial plasma medium fabricated by an array of thin conducting wires. The radiation pattern of plain and corner plasma reflector antennas modeled using Drude equations are obtained and are compared with a plasma reflector and conventional metallic reflector antennas. The results obtained for the plasma reflector antenna is experimentally verified using a 90° corner reflector antenna fabricated using wire medium. This new class of plasma antennas show marked variations in radiation pattern for frequencies above and below plasma frequency, which may find potential use in various frequency selective applications.

Keywords: negative permittivity, FDTD, dispersive medium, artificial plasma, reflector antenna, metamaterials

(Some figures may appear in colour only in the online journal)

1. Introduction

Metamaterials are artificially fabricated composites that exhibit unusual and unique electromagnetic properties due to negative values for permittivity, permeability and refractive index. This new class of materials was first proposed by Russian physicist Victor G. Veselago in 1968 [1]. In the beginning of this millennium, the proposed medium was realized in the form of a bulk medium by the periodic arrangement of structures having intrinsic negative values of permittivity and permeability. It was Pendry *et al* who, for the first time, realized both these negative permittivity and permeability materials using a periodic array of thin conducting wires and split ring resonators (SRRs) in 1996 and 1999 respectively [2, 3]. By combining both these structures in a specialized manner, the negative refractive index medium, also called the backward wave medium or left-handed medium (LHM), was actualized in the year 2000 by Smith and his colleagues for microwave frequencies [4]. Since the periodicity of the constituent metamolecules in the composite is very much less than the interacting wavelength, the medium exhibits homogeneous properties. Owing to their exotic characteristics such as the reversal of Snell's law, inverse Doppler effect, cloaking etc shown by this group of materials, immense research is going on in this field for a wide variety of applications for the support of the state of the art technology. Active research is taking place for realizing different variants of both single negative (SNG) and double negative (DNG) metamaterials for a wide variety of applications like

[1] Vimala College (Autonomous), Thrissur, University of Calicut, Kerala, India.
[2] St. Thomas' College (Autonomous), Thrissur, University of Calicut, Kerala, India.

sensors, frequency selective surfaces, miniaturized antennas and material characterization studies [5–10] .

The epsilon negative (ENG) medium, one constituent part of the SNG metamatrials, has gained importance in microwave and terahertz research fields due to its frequency selective properties. The possibility of materializing the above medium by various artificial methods has been explored by different researchers in recent years. One of the easiest methods proposed to realize the above mentioned artificial plasma medium is by employing a periodic array of thin conducting wires [11, 12]. Depending upon the periodicity and the radius of the wire employed, the plasma frequency of the medium can be tuned to any desired value.

Even though the electron concentration is confined to the region of conducting wires employed to make the epsilon negative medium, it will act as a homogeneous medium since the periodicity of wires is much less than the wavelength of the interacting electromagnetic wave. This ENG medium will show frequency-dependent radiation properties in relation to the effective electron density, which will be the averaged electron density value obtained by distributing the electrons confined in the region of metalization to the entire medium space. Since the effective average electron density is a function of conductivity of material employed to make the wire and its periodicity in making the artificial ENG wire medium, we can vary the plasma frequency in an accurate manner. Since this frequency selective property of the plasma medium does not depend on a resistive absorption mechanism resulting in an ohmic power loss which, in fact, is one of the major factor contributing to the frequency selectivity of most of the microwave frequency selective absorbers reported in the literature [9], the distinct advantage and importance of employing the ENG medium for frequency selective-based devices is quite obvious. In other words, the plasma type frequency selective medium will act as a window for the incoming electromagnetic power by transmitting or reflecting the wave based on the intrinsic plasma frequency, whereas the other commonly used microwave absorbers will act as a dissipation medium often in a wide band of frequencies.

This dispersive artificial plasma medium can be effectively modeled using the finite difference time domain (FDTD) method [13, 14]. The two possible ways for modeling these media are by the periodic insertion of the thin conducting wires in the medium and by considering it as an effective medium. Out of the three major dispersive FDTD methods—the auxiliary differential equation method (ADE), the recursive convolution method (RC) and the Z transform method—ADE is commonly used to model metamaterial-related electromagnetic problems [13, 15–17].

In this paper, we have employed the two-dimensional ADE-FDTD method to model frequency dependent reflector antennas using negative permittivity plasma slabs making use of the effective medium theory. Initially we have modeled an artificial plasma medium and its frequency-dependent behavior is analyzed using a Gaussian pulse. The results are experimentally verified by fabricating an artificial ENG sheet using an array of thin copper wires. A host of applications in the microwave regime is materialized using antennas having

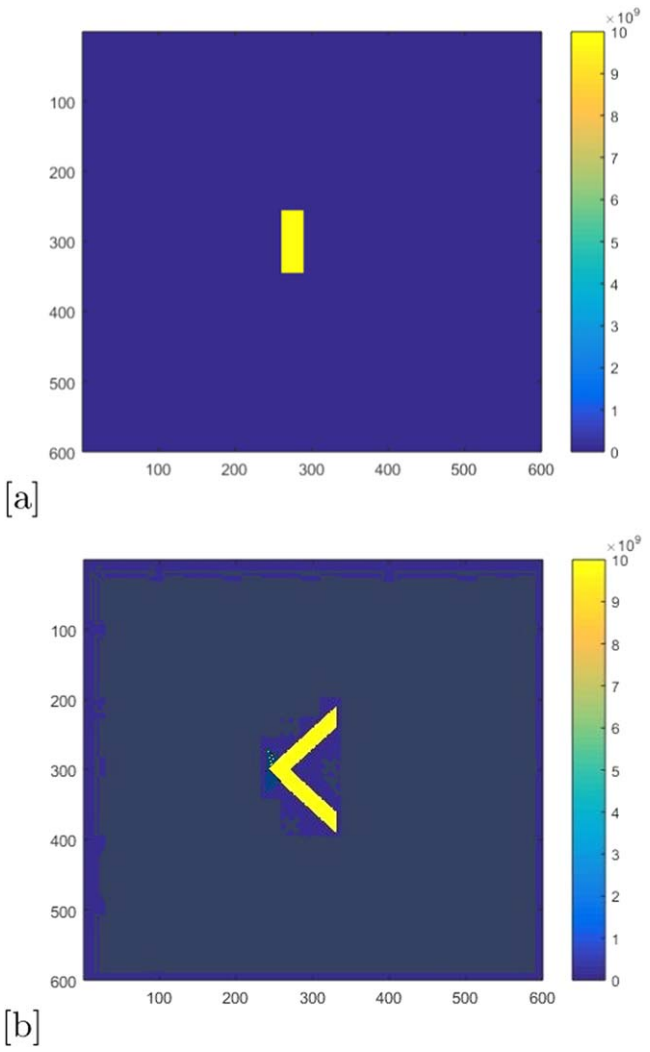

Figure 1. Positioning of the negative permittivity reflector antenna in the computational domain for (a) the plane reflector and (b) the corner reflector.

properties like frequency independence, frequency selectivity and frequency tunability.

Since radiation pattern is one of the major characteristics of any type of antenna, the studies related to the radiation pattern modification for specific application is a topic of interest for antenna engineering researchers. The requirements, like multiband radiating frequencies even with distinct radiation patterns, make the fast-emerging meta-inspired research area open to a new arena in the field of antenna applications. For example, Joe *et al* has recently proposed a featherlight horn antenna, which may have potential applications in astronomical and communication fields using the concept of the ENG wire medium [10]. Horn antennas, reflector antennas and microstrip antennas are often tried to realize frequency selective and frequency tunable applications [18].

In this paper, we are introducing a reflector antenna having frequency selective characteristics that exhibit different radiation behaviors at selected working frequencies using the principle of the ENG medium. Reflector antennas of

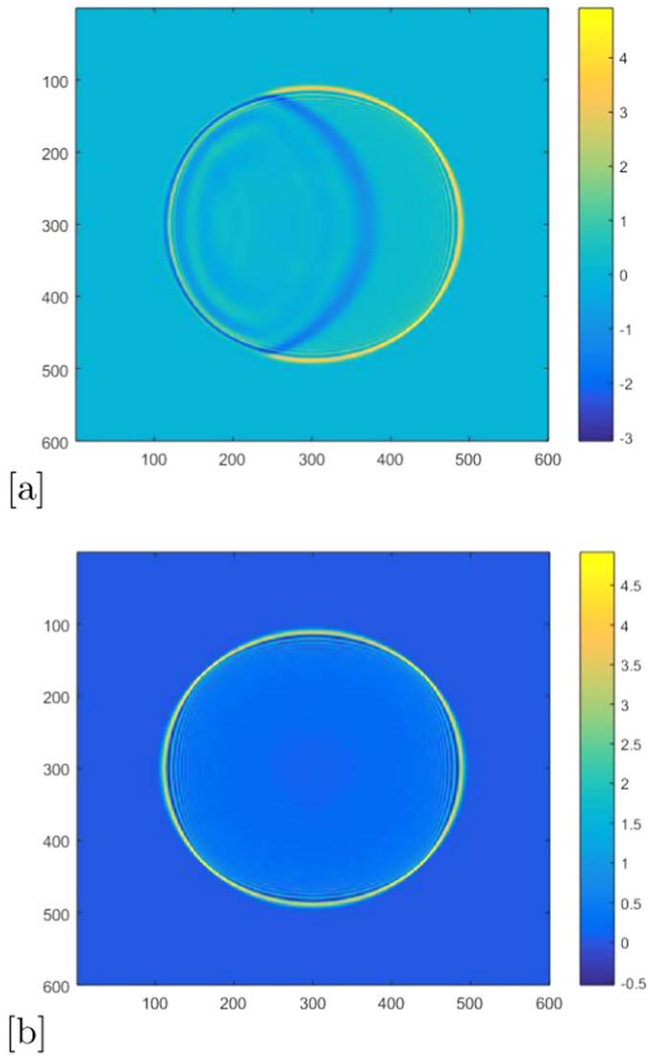

Figure 2. Propagation of the Gaussian pulse through the work space (a) in the presence of the negative permittivity slab (placed between x = 260 and 290, y = 260 and 340) and (b) in the absence of the slab. The excitation point is at $x = 310$, $y = 300$.

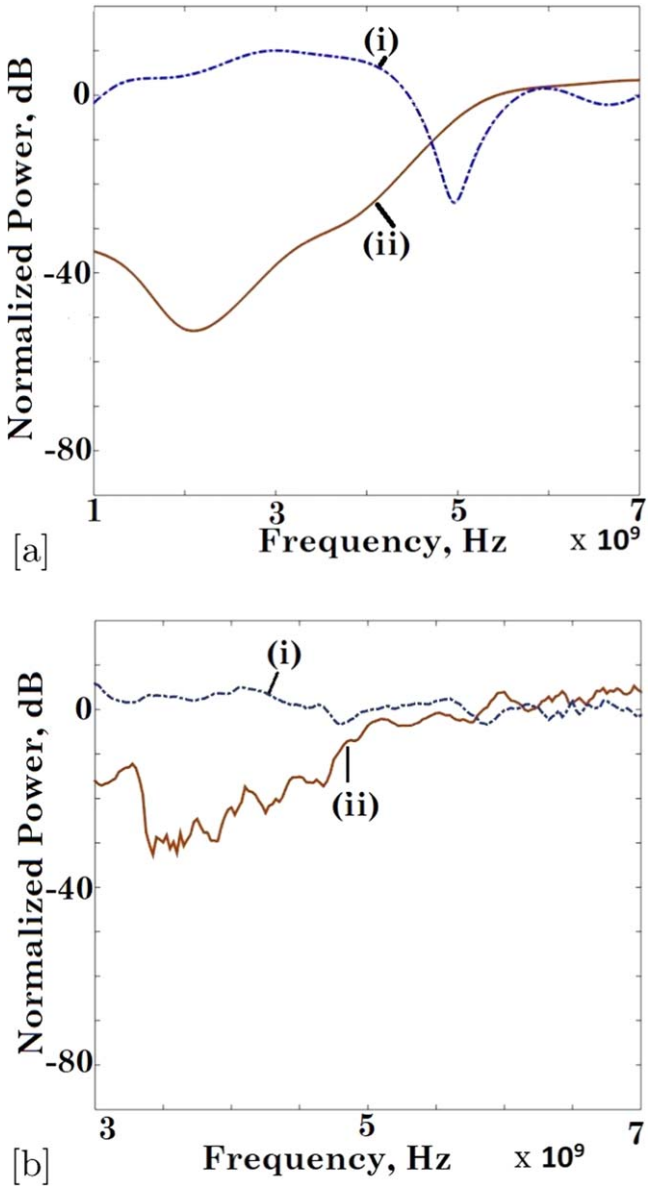

Figure 3. Normalized power densities obtained by (a) simulation and (b) experiment at two points in the presence of the plasma slab - (i) in the same side of the slab and (ii) behind the slab.

different geometries are quite popular in various microwave applications [18] and, in our present work, we are realizing a novel type of metamaterial-inspired reflector antenna using an artificially engineered negative permittivity plasma medium. Since plasma medium exhibits some intrinsic propagation and reflection properties in relation to its plasma frequency, the reflector antenna designed using this medium will follow the desired frequency selective characteristics. The performance of this plasma reflector antenna is compared with the conventional metallic reflector antenna and the results are analyzed. The plasma frequency-related selective properties are clearly observed in the radiation characteristics of this new reflector antenna.

2. Formulation of the problem

In order to model the plasma medium using effective medium theory we have used the Drude model equations in the 2D ADE-FDTD method. The relative permeability $\mu_r(\omega)$ and the relative permittivity $\epsilon_r(\omega)$ for this model are given by,

$$\mu_r(\omega) = 1 - \frac{\omega_{mp}^2}{\omega^2 - \omega_{m0}^2 - i\gamma_m\omega} \tag{1}$$

$$\epsilon_r(\omega) = 1 - \frac{\omega_{ep}^2}{\omega^2 - \omega_{e0}^2 - i\gamma_e\omega} \tag{2}$$

where ω_{ep} and ω_{mp} are the electric and magnetic plasma frequencies, ω_{e0} and ω_{m0} are the low frequency edge of the electric and magnetic forbidden bands, and γ_e and γ_m are the electric and magnetic damping factors. The transverse magnetic wave components (TM) E_z, H_x and H_y of Maxwell' s equations are given by,

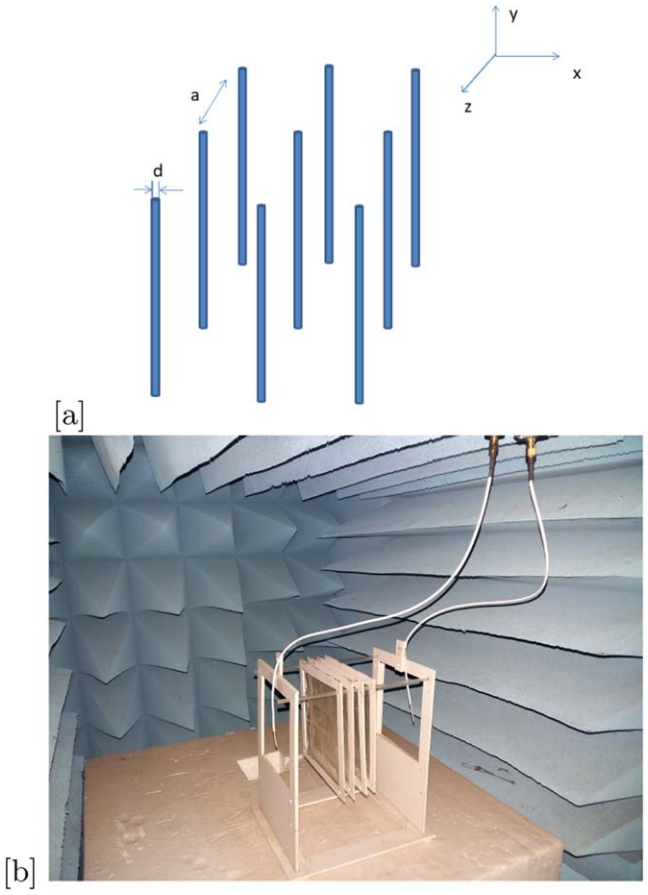

Figure 4. (a) The schematic representation of the wire medium showing the diameter 'd' and periodicity 'a' (b) Experimental setup used to study the field distribution near the artificial plasma slab.

$$\frac{\partial D_z}{\partial t} = \frac{\partial H_y}{\partial x} - \frac{\partial H_x}{\partial y} \tag{3}$$

$$\frac{\partial B_x}{\partial t} = -\frac{\partial E_z}{\partial y} \tag{4}$$

and

$$\frac{\partial B_y}{\partial t} = \frac{\partial E_z}{\partial x}. \tag{5}$$

Since the medium under consideration is dispersive, E_z, H_x and H_y are expressed in terms of D and B using the Drude model as [13],

$$D_z = \epsilon_0\left(1 - \frac{\omega_{ep}^2}{\omega^2 - \omega_{e0}^2 - i\gamma_e\omega}\right)E_z \tag{6}$$

$$B_x = \mu_0\left(1 - \frac{\omega_{mp}^2}{\omega^2 - \omega_{m0}^2 - i\gamma_m\omega}\right)H_x \tag{7}$$

$$B_y = \mu_0\left(1 - \frac{\omega_{mp}^2}{\omega^2 - \omega_{m0}^2 - i\gamma_m\omega}\right)H_y. \tag{8}$$

For modeling the ENG medium, we convert equations (6)–(8) from the frequency domain to the time domain by replacing $i\omega$ by $\partial/\partial t$ and applying the second-order FDTD discretization in space and time [19].

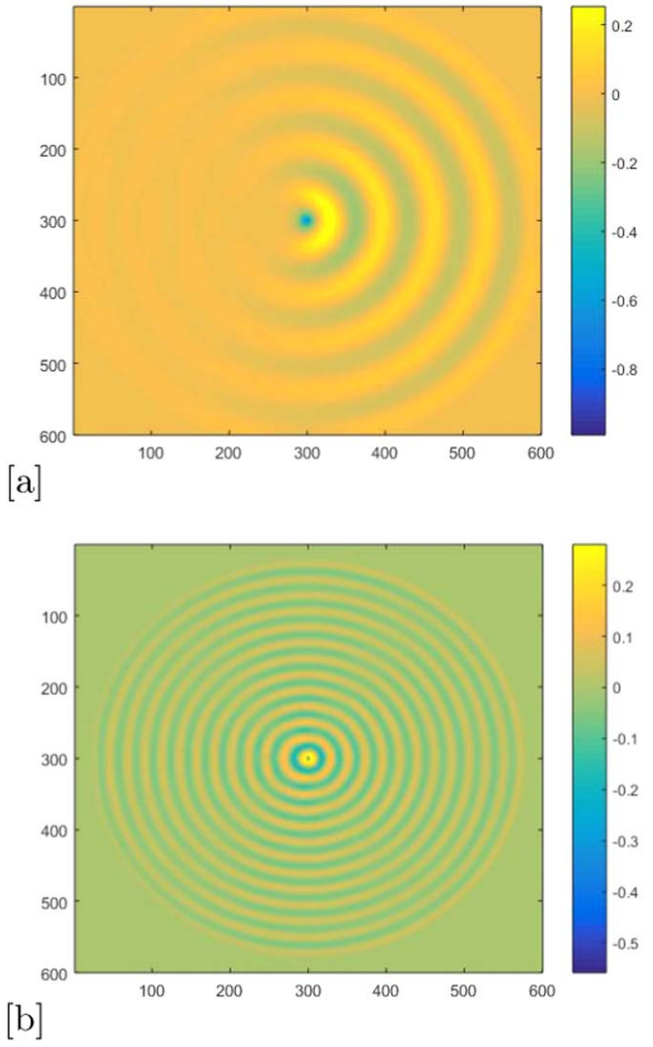

Figure 5. Propagation of sine pulse in the presence of the plasma plane reflector antenna through the computational domain for (a) 3 GHz and (b) 9 GHz.

The domain space selected for the modeling is of dimensions 600 × 600 cells where each grid is of size 1.5 mm (figure 1). The rectangular and corner shaped patches seen in the above figures 1(a) and (b) corresponds to the ENG reflector structure in the computational domain. The time step used for the simulation is set as $\Delta t = \Delta x/\sqrt{2}\,c$. Negative permittivity reflector antennas are constructed in the above computational space by setting ω_{ep} with a typical value 4.5 GHz for the plasma region and zero for the remaining portion. ω_{mp} is set as zero for the entire space.

3. Designing of the plasma slab

The plasma frequency-related transmission properties of the plasma slab used for making the reflector antenna is analyzed by simulation using effective medium theory and confirmed by experiment. For simulation, a plasma slab of dimension 30 × 80 cells is used. An excitation source in the form of a Gaussian pulse is allowed to propagate through the

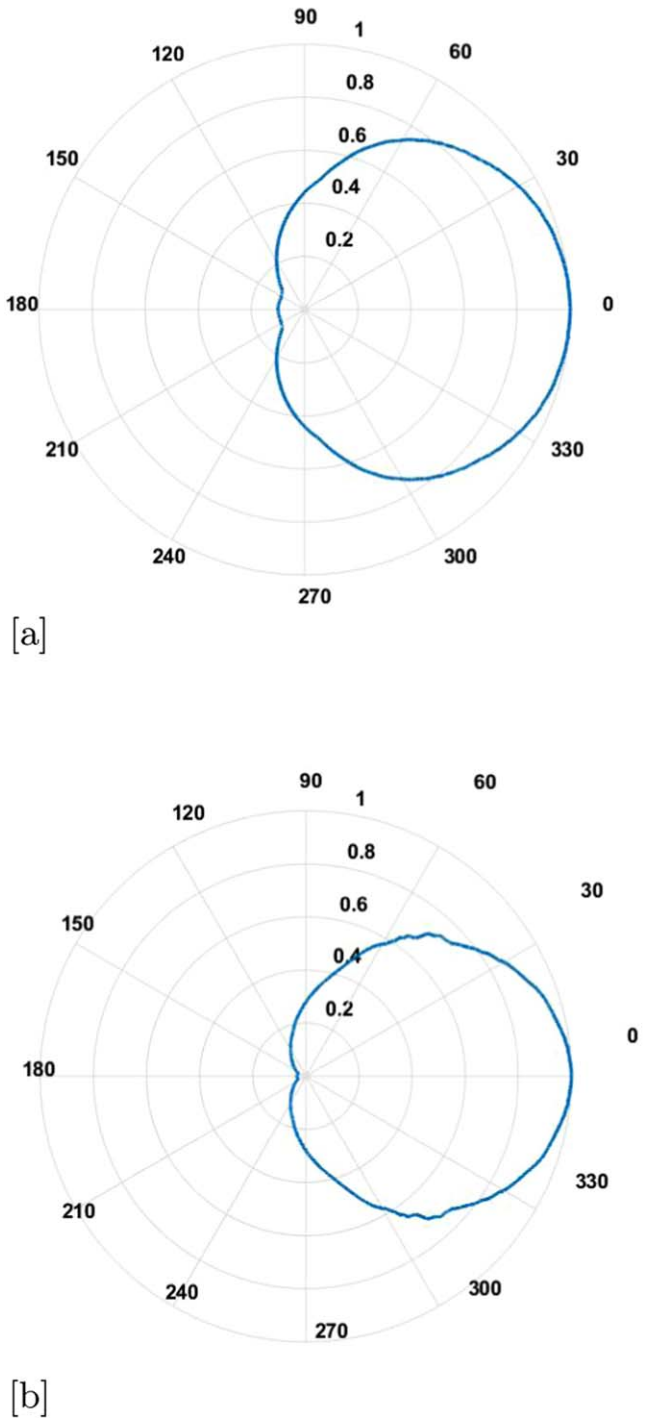

Figure 6. Simulated radiation pattern for 3 GHz. (a) The plasma slab reflector and (b) the metal slab reflector.

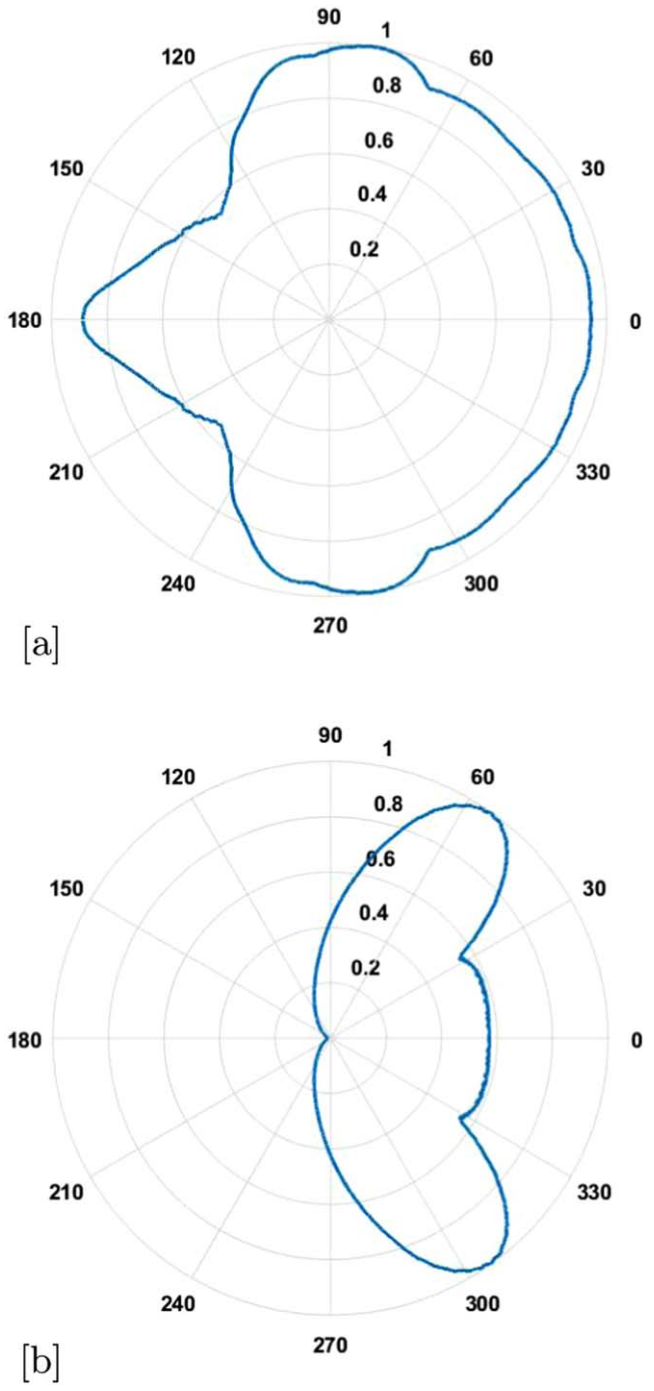

Figure 7. Simulated radiation pattern for 9 GHz. (a) The plasma slab and (b) the metal slab reflector.

computational domain. Electrical plasma frequency of the slab is selected as 4.5 GHz. The propagation of the Gaussian pulse in the computational domain with and without the presence of plasma slab is shown in figures 2(a) and (b). The field intensities of the above two cases are measured at two points, which are on both sides of the slab, along the axis and the corresponding Fourier transforms after normalizations are plotted in figure 3(a). It is clear that all frequencies are present when the measurement is taken in the same side of the slab at $x = 390$ and $y = 300$ (Curve *i*). The lowering of the power at certain frequencies on the curve may be explained in terms of the destructive interference of the field with the reflected part due to the $\lambda/2$ dependent separation of the source from the slab. On the other side of the slab correspondingly $x = 230$ and $y = 300$, only frequencies above the plasma frequency are present with noticeable magnitude (Curve *ii*).

For experimental verification of the above result, an artificial ENG slab is designed using a wire medium having different layers as depicted in figure 4(a).The diameter of wire is 'd' and its periodicity is 'a'. Plasma frequency (f_p) of the

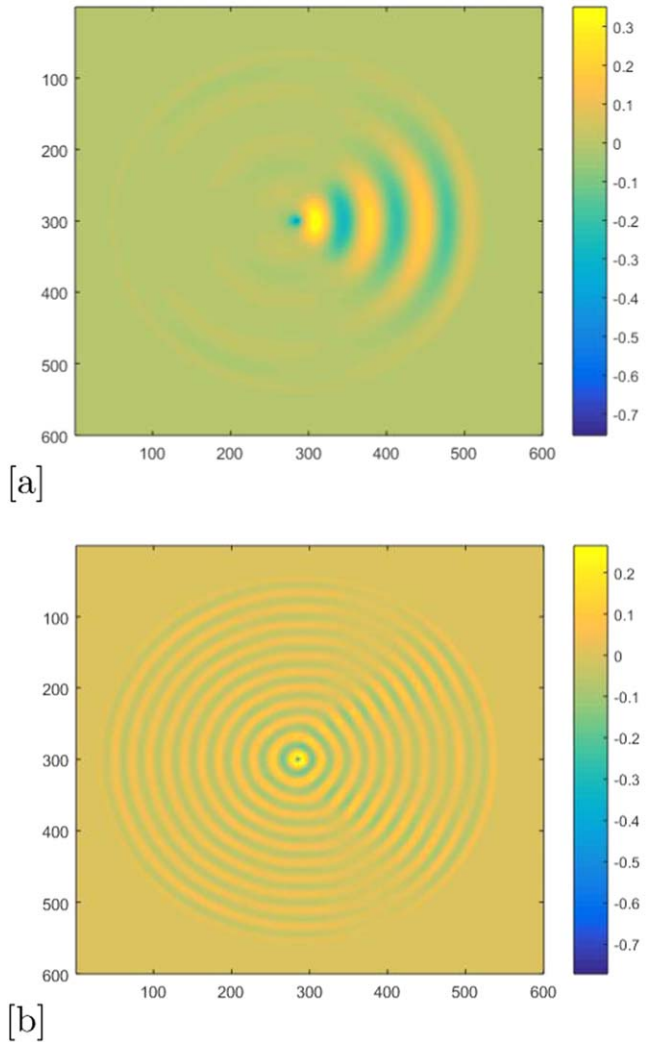

Figure 8. Propagation of sine pulse in presence of the plasma corner reflector antenna through the computational domain for (a) 3 GHz and (b) 9 GHz.

wire medium is given by [12]

$$f_p = \frac{c}{a\sqrt{2\pi \ln(\frac{2a}{d})}} \tag{9}$$

where 'c' is the velocity of light. We have fabricated an artificial plasma slab for the above plasma frequency (4.5 GHz) using thin copper wires and verified its transmission properties experimentally with the purpose of using it in the proposed reflector antenna [11]. Copper wires of radius 0.027 mm are used to make plasma sheets by arranging them 1.1 cm apart on a frame made of a low loss PVC foam sheet. Four such frames are arranged with the spacing of 1.3 cm for materializing a plasma medium. Theoretical plasma frequency for this artificial medium is 4.5 GHz [20]. The wave propagation properties of this slab are analyzed by placing it between microwave transmitting and receiving probes connected to a vector network analyzer (VNA). The distance between the transmitting probe and the plasma slab is set as 3 cm. The photograph of the experimental arrangement inside the anechoic test box is shown in figure 4(b). The measured

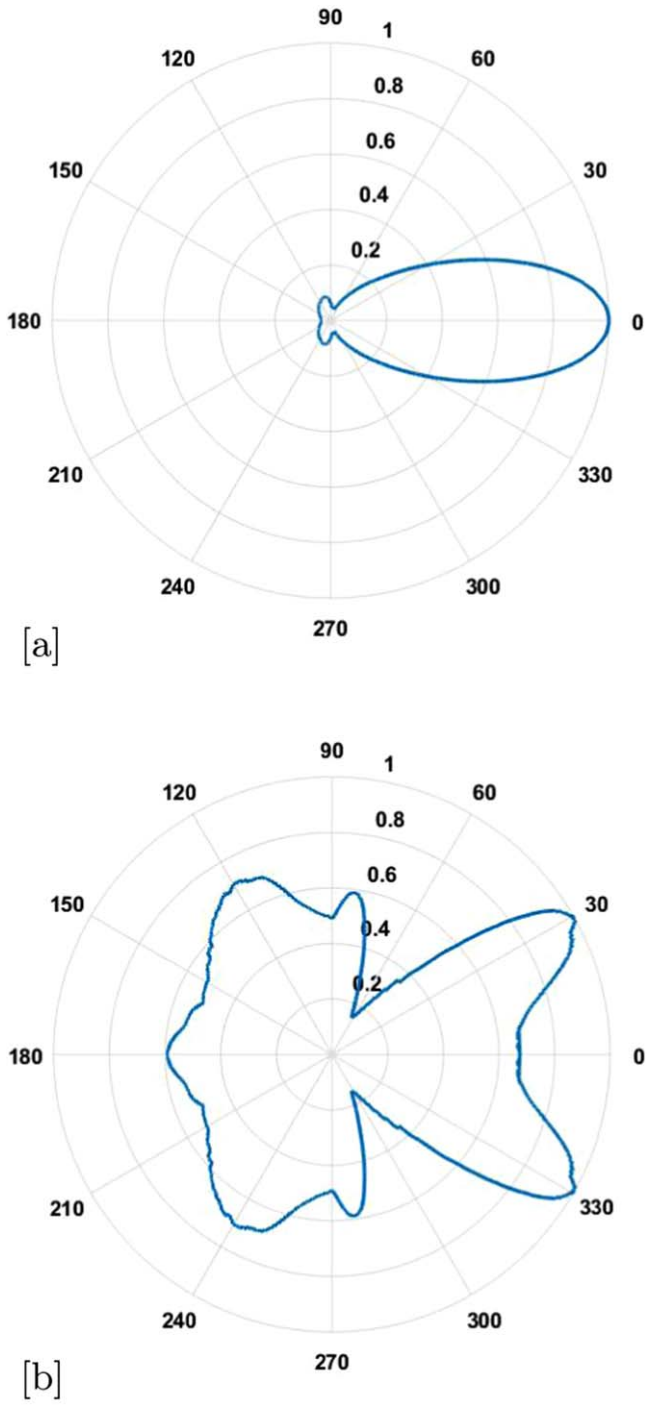

Figure 9. Simulated radiation pattern of the 90° plasma corner antenna for (a) 3 GHz and (b) 9 GHz.

power on both sides of the slab at a distance of 12 cm from the transmitting probe for a frequency sweep of 3–7 GHzs is plotted in figure 3(b). As expected, in the same side of the plasma slab almost all frequencies are present (Curve *i*) and, on the back side, reflector frequencies below plasma frequency are absent (Curve *ii*).

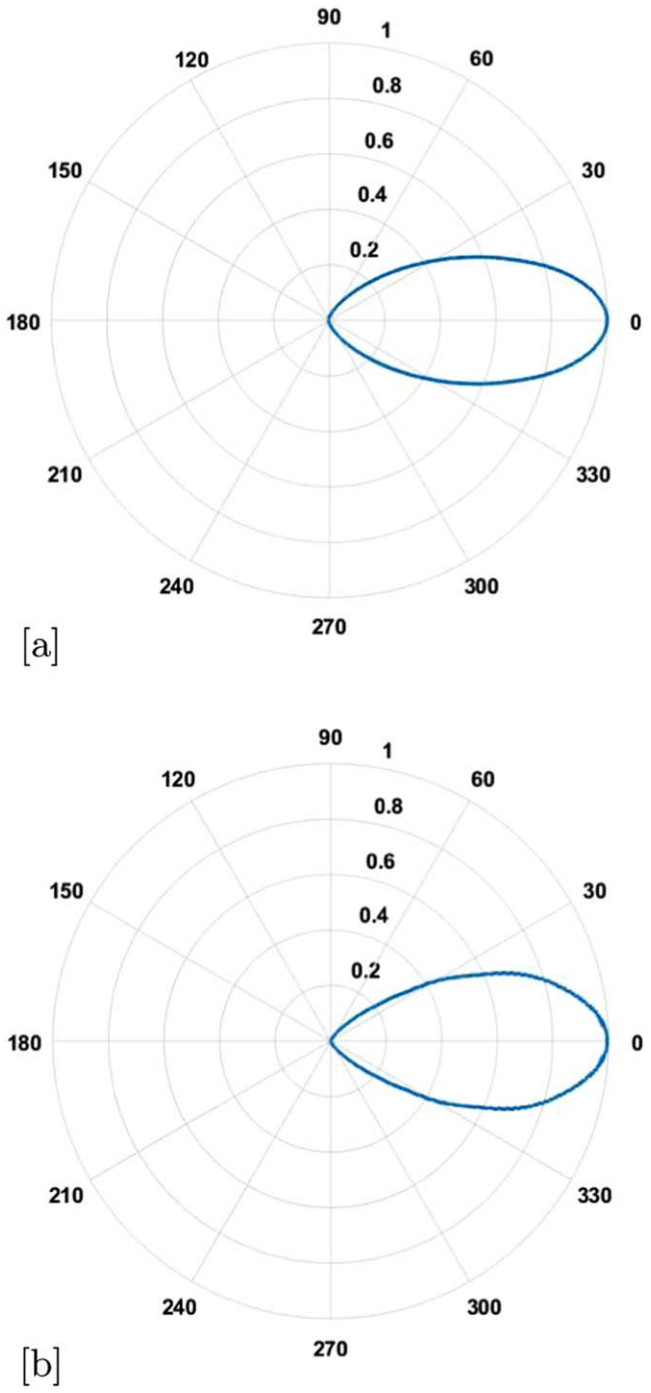

Figure 10. Simulated radiation pattern of the 90° metal corner antenna for (a) 3 GHz and (b) 9 GHz.

4. Plasma reflector antenna: design, simulation and experimental verification

The frequency-dependent radiation characteristics of the proposed reflector antenna is realized both by FDTD simulation and by experiment using the already modeled plasma medium. Two specific designs chosen were the plane reflector and a 90° corner reflector antenna, and the positioning of these reflectors in the computational domain are shown in figure 1. For the plane reflector, a plasma slab of thickness

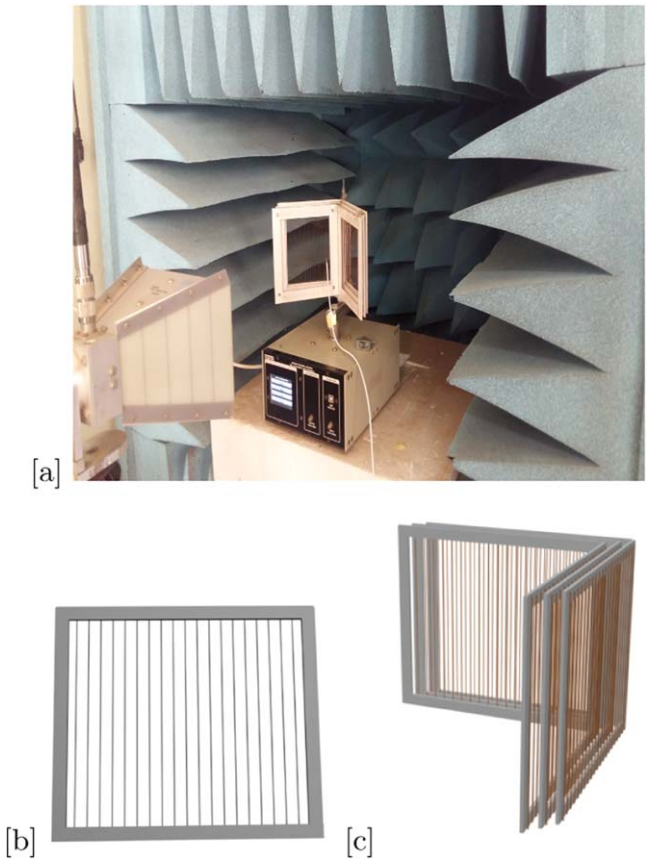

Figure 11. (a) Experimental setup to study the radiation pattern of the plasma corner reflector antenna, (b) schematic diagram of the plasma sheet used to fabricate the slab and (c) schematic representation of the plasma corner reflector antenna.

45 mm and length 120 mm is placed in the domain between $x = 260$ and 290, $y = 260$ and 340. The 90° corner reflector antenna is realized by placing two slabs of thickness 30 mm and length 120 mm with slopes of $+45°$ and $-45°$ to the horizontal with respect to the vertex at $x = 300$ and $y = 270$. We have selected two typical frequencies, one below the plasma frequency (3 GHz) and the other above the plasma frequency (9 GHz) and have allowed the wave to propagate through this domain to validitate the frequency selective nature. For the plane reflector, the field distributions obtained for frequencies 3 GHz and 9 GHz are shown in figures 5(a) and (b) respectively. For frequency less than the plasma frequency (figure 5(a)), we get the field distribution only in the right side of the reflector, whereas for the frequency greater than the plasma frequency (figure 5(b)) we get transmission patterns on both sides of the reflector. In order to analyze the radiation pattern we take the field distribution in the $X - Y$ plane at a radial distance of 200 grid length from the center of the plasma slab in-line with the source point. Figure 6(a) is the polar plot for 3 GHz, which is well below the plasma frequency and from the pattern it is clearly evident that the intensity distribution at the rear side is negligibly small. Figure 6(b) shows the radiation pattern obtained by simulation after replacing the plasma slab with a metal reflector of the same dimensions and the obtained pattern are almost

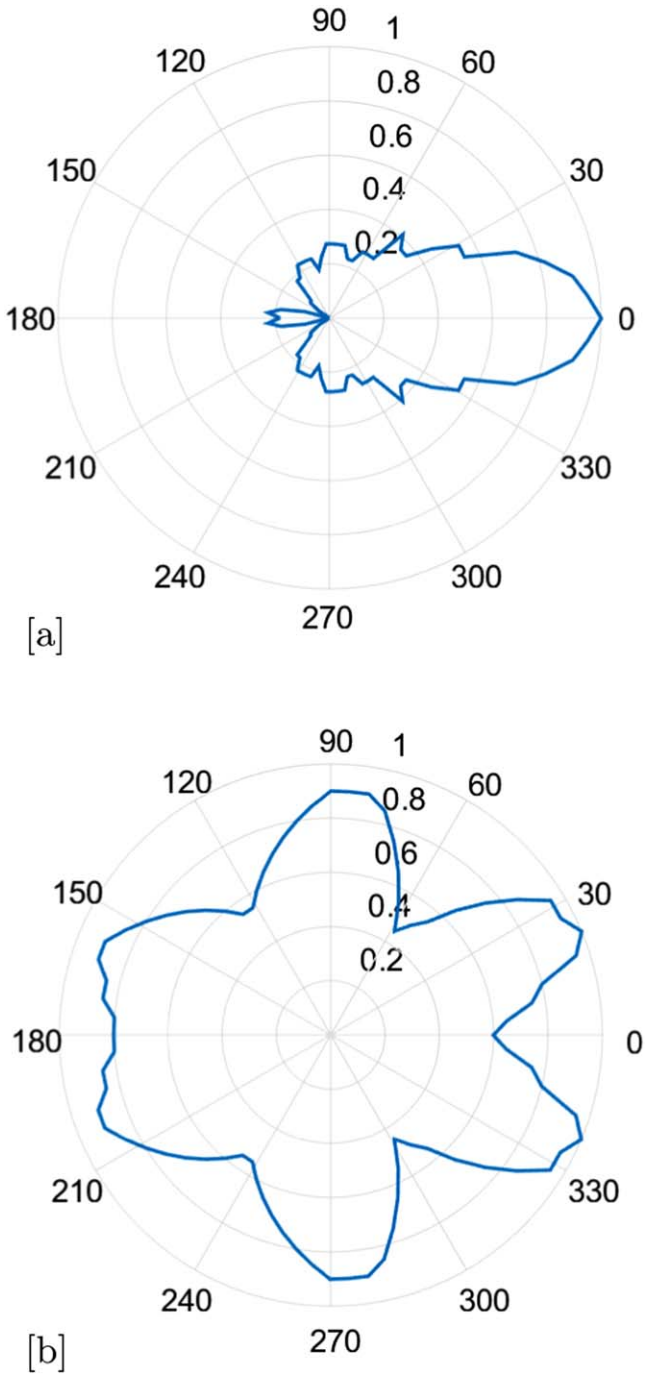

Figure 12. Experimental radiation pattern of the 90° plasma corner antenna for (a) 3 GHz and (b) 9 GHz.

identical. Figure 7(a) is for 9 GHz, which is well above the plasma frequency and as is expected the field propagation through plasma medium is quite vivid. Figure 7(b) shows a corresponding simulation plot for an equivalent metallic reflector and as expected we obtain a comparably strong field intensity only on the right side of the metallic reflector. From the above results, it is evident that the proposed plane plasma reflector antenna exhibits remarkable deviation from its metallic counterpart in relation to the plasma frequency.

We have also carried out the radiation behavior of 90° plasma corner reflector antenna. Here also two fixed frequencies, 3 GHz and 9 GHz, which are above and below the plasma frequency are allowed to propagate through the computational space and the corresponding field distributions are shown in figures 8(a) and (b). For 3 GHz as in figure 5(a), the plasma corner reflector antenna also behaves like a metal reflector, whereas for 9 GHz as in figure 5(b), it shows a field distribution in the entire work space owing to its plasma properties. Radiation patterns are plotted from the field distribution as for the case of the plane reflector. Figures 9(a) and (b) shows the pattern for the 90° plasma reflector corresponding to 3 GHz and 9 GHz respectively and the similar patterns obtained by simulation for their metallic counterparts are given in figures 10(a) and (b). It is quite evident for 9 GHz that there is a clear distinction in radiation pattern between the metallic and the plasma structures confirming the frequency dependent plasma characteristics of this novel reflector antenna. For further verification, the radiation patterns of the plasma reflector is plotted experimentally with a turntable setup and the photograph of the experimental arrangement is shown in figure 11(a) along with the schematic representation of the plasma sheet used for the fabrication of the slab (fig 11(b)) and the corner reflector antenna (figure 11(c)). The corner reflector antenna is constructed by employing two sets of plasma slabs used for the experimental study of the near field distribution (figure 4) kept at an angle of 90°. The source is placed at a distance of 1λ from the vertex of the antenna. Figures 12(a) and (b) shows the radiation patterns obtained for the plasma corner reflector antenna for frequencies 3 GHz and 9 GHz. As it is evident from figure 12(b), for the experimental case a clear distinction is also observed in the radiation pattern of the plasma corner reflector antenna from its metallic counterpart for frequencies above the plasma frequency.

5. Conclusion

A negative permittivity metamaterial-based artificial plasma reflector antenna is presented and its frequency-dependent radiation patterns are presented both by simulation and experiment. The 2D-ADE FDTD method is employed for simulation by considering the plasma slab as an effective medium. The transmission properties of the plasma slab is analyzed using the above simulation method and the results obtained are verified experimentally by fabricating a plasma slab using thin copper wires. By employing the plasma slab, the corner reflector antenna exhibiting frequency-dependent radiation characteristics is fabricated for the first time and its field patterns are measured. The results are found to be in quite good agreement with that obtained by FDTD simulation. It is evident that by proper arrangement the plasma slab can be effectively used as a frequency-dependent reflector antenna.

Acknowledgments

Jovia Jose gratefully acknowledges the University Grant Commission (UGC) of India for the financial support under the Faculty Development Programme.

ORCID iDs

V P Joseph https://orcid.org/0000-0001-5501-0220

References

[1] Veselago V G 1968 *Soviet Physics Uspekhi* **10** 509
[2] Pendry J B, Holden A, Stewart W and Youngs I 1996 *Phys. Rev. Lett.* **76** 4773
[3] Pendry J B, Holden A J, Robbins D and Stewart W 1999 *IEEE Trans. Microwave Theory Tech.* **47** 2075
[4] Smith D R, Padilla W J, Vier D, Nemat-Nasser S C and Schultz S 2000 *Phys. Rev. Lett.* **84** 4184
[5] Chakyar S P, Simon S K, Bindu C, Andrews J and Joseph V P 2017 *J. Appl. Phys.* **121** 054101
[6] Ragi P M, Umadevi K S, Nees P, Jose J, Keerthy M V and Joseph V P 2012 *Microwave Opt. Technol. Lett.* **54** 1415
[7] Sikha Simon K, Chakyar S P, Andrews J and Joseph P V 2017 *in American Institute of Physics Conference Series* **1849** 020021
[8] Umadevi K, Chakyar S P, Simon S K, Andrews J and Joseph V 2017 *EPL (Europhysics Letters)* **118** 24002
[9] Paul N, Chakyar S P, Umadevi K, Sikha S K, Kizhakooden J, Andrews J and Joseph V 2019 *Arab. J. Sci. Eng.* **44** 553
[10] Kizhakooden J, Jose J, Paul N, Simon S K, Chakyar S P, Andrews J and Joseph V 2018 *Microwave Opt. Technol. Lett.* **61** 777–80
[11] Ivzhenko L 2016 *II International Young Scientists Forum onApplied Physics and Engineering (YSF) (IEEE)* 88–91
[12] Pendry J B, Holden A, Robbins D and Stewart W 1998 *J. Phys. Condens. Matter* **10** 4785
[13] Taflove A and Hagness S C 2005 *Computational Electromagnetics: The Finite-Difference Time-Domain Method* (Norwood, MA: Artech House)
[14] Jose J, Chakyar S P, Andrews J and Joseph V 2016 *Numerical Electromagnetic and Multiphysics Modeling and Optimization (NEMO), 2016 IEEE MTT-S International Conference on (IEEE)* pp 1–3
[15] Lee J-Y, Lee J-H, Kim H-S, Kang N-W and Jung H-K 2005 *IEEE Trans. Magn.* **41** 1484
[16] Kashiwa T, Yoshida N and Fukai I 1990 *Antennas and Propagation Society International Symposium, 1990. AP-S. Merging Technologies for the 90's. Digest. (IEEE)* 1656–9
[17] Sullivan D M 2013 *Electromagnetic Simulation Using the FDTD Method* (New York: Wiley)
[18] Johnson R C and Jasik H 1984 *Antenna Engineering Handbook* (New York: McGraw-Hill Book Company)
[19] Hao Y and Mittra R 2008 *FDTD Modeling of Metamaterials: Theory and Applications* (Boston, London: Artech House)
[20] Simovski C R, Belov P A, Atrashchenko A V and Kivshar Y S 2012 *Adv. Mater.* **24** 4229